Exergy-based sizing of a R290 air-to-water reversible heat pump for space heating and cooling purposes

Volodymyr Voloshchuk[a], Paride Gullo[b], Oleksandr Stepanets[c] and Eugene Nikiforovich[d]

[a] National Technical University of Ukraine "Igor Sikorsky Kyiv Polytechnic Institute", Kyiv, Ukraine, vl.volodya@gmail.com
[b] University of Southern Denmark (SDU), Department of Mechanical and Electrical Engineering, Sønderborg, Denmark, parigul@sdu.dk
[c] National Technical University of Ukraine "Igor Sikorsky Kyiv Polytechnic Institute", Kyiv, Ukraine, stepanets.av@gmail.com
[d] National Technical University of Ukraine "Igor Sikorsky Kyiv Polytechnic Institute", Kyiv, Ukraine, eugnik@gmail.com

Abstract:

This works aims at evaluating the impact of different ratios of heating design loads to cooling ones on the thermodynamic efficiency of a R290 air-to-water reversible heat pump with the aid of an exergy analysis. The potential improvements of the investigated solution were also assessed. The heat pump was sized for a two-pipe fan-coil system designed with supply/return water temperatures of 45/40 °C in winter and 7/12 °C in summer. The outdoor air was cooled from -7 ℃ to -12 ℃ in heating mode and heated from 30 ℃ up to 35 ℃ in cooling mode, respectively. The heating loads were varied in a range from 8 kW to 13 kW, whereas the cooling loads were ranged between 6 kW and 15 kW, respectively.

The results obtained showed that heat exchanger sizing plays a significant impact on the distribution of exergy destruction within the system components. As the system was sized based on the cooling load, the air-based heat exchanger was found to be oversized and the water-based heat exchanger was observed to be undersized for covering the heating loads and vice versa. It was also found that for the ratios of heating design loads and cooling ones less than 1.2 the system should be sized based on the cooling design loads. In this case lower system exergy destruction could be obtained. Furthermore, in this case the thermodynamic improvement of the air-based heat exchanger, the water-based heat exchanger and the compressor had approximately the same potential of increasing the efficiency of the system. As the ratios of heating design loads and cooling ones were higher than 1.2, the heating load should have been used for sizing the system components due to higher thermodynamic efficiency of the system compared to the previous case and technical possibilities to be operated. Removing the avoidable irreversibilities within the air-based heat exchanger offered the biggest decrease of the exergy destruction within the system.

Keywords:

Exergetic analysis; Exergy destruction; Heat pump; Propane; Thermodynamic enhancement.

1. Introduction

Today a large offer of reversible heat pumps with investment costs comparable to those of non-reversible units is available. These solutions are one of the most widely used heating, ventilation and air conditioning (HVAC) technologies in Europe. About 70 % of air-conditioned office buildings are cooled down by reversible heat pumps [1]. Such units have the ability to provide low carbon heating and cooling and great thermal comfort levels through one distribution system (assuming the emitter is capable of providing both modes).

During the last decades the research has demonstrated the impact of refrigerants on ozone depletion and global warming. So, the implementation of highly thermodynamically efficient heat pumps relying on very low global warming potential (GWP) refrigerants is compulsory.

The authors of [2] dealt with a numerical analysis of a reversible air-source heat pump incorporated into the HVAC system of a typical office building. The results obtained showed that energy performance of the system strongly depended on the of the unbalance indicator, estimated as the ratio of cooling loads to heating ones of the building, and of the overall index of heat pump oversizing/downsizing with respect to the design loads of the building.

https://doi.org/10.52202/069564-0077

In [3] the simulation model of an air-to-water R410A based reversible heat pump was developed to simulate its performance at off design conditions. The annual efficiency of the system was found to be able to be maximized by changing temperature, flow rate of air and water and refrigerant mass flow rate.

The relationship between air-to-water heat pump performance using R410A and the Italian building heating and cooling loads was numerically investigated by Madonna et al. [4]. The authors observed that the reversible heat pump oversizing can cause an excessive on/off cycling and an efficiency reduction (up to 25 %).

Most of current heat pumps use hydrofluorocarbons (HFCs), which have a massive GWP. Therefore, in the last decade several studies have been devoted to investigate environmentally friendlier alternatives, e.g. hydrofluoroolefins (HFOs) [5] and hydrocarbons (HFC) [6]. However, the recent environmental concerns on HFOs are promoting the adoption of natural refrigerants. In addition, [6] observed that R290 is a better substitute for R134a than R600a for residential heat pump water heaters.

From the review made above, it is possible to conclude that the reversible heat pump sizing strongly affects energy efficiency of such systems. Most of the investigations has been based on analyses focusing on conventional objective variables and conventional energy assessments. However, application of exergy analysis would provide better insight into possibilities to reveal the location, the magnitude and the sources of thermodynamic inefficiencies within the system. Advanced exergy analysis additionally considers thermodynamic interactions among components and the real potential for the system improving. Investigations of reversible heat pumps with ultra-low GWP refrigerants are also of high interest. Thus, the goal of this work is to bridge this knowledge gap by applying the exergy methodology for sizing an air-to-water reversible heat pump with propane and evaluating the real potential for its thermodynamic improvement.

2. Materials and Methods

2.1. Conventional Exergy Analysis

In the conventional exergetic evaluation of the k-th component of the investigated system, the following equations were used [7]:

- Gouy–Stodola theorem

$$\dot{E}_{D,k} = T_0 \dot{S}_{gen,k}, \qquad (1)$$

where $\dot{E}_{D,k}$ is exergy destruction rate within the k-th component, T_0 is temperature of the reference environment and $\dot{S}_{gen,k}$ is the entropy generation owing to internal irreversibilities;

- the exergy balance for the k-th component

$$\dot{E}_{F,k} = \dot{E}_{P,k} + \dot{E}_{D,k}, \qquad (2)$$

where $\dot{E}_{F,k}$ and $\dot{E}_{P,k}$ are exergy rates associated with fuel and product of the component, respectively.

2.2. Evaluation of Removable Exergy Destruction

Since evaluating removable parts of exergy destruction occurring in each system component was within the scope of the work the method presented in [8] was applied. According to this method, the avoidable exergy destruction rate ($\dot{E}_{D,k}^{AV,INT}$), which is internally caused, can be computed as the difference between the total exergy destruction of the investigated component ($\dot{E}_{D,k}$), i.e., calculated under real operation conditions, and its exergy destruction ($\dot{E}_{D,k}^{MIN,k}$) evaluated under conditions at which its irreversibilities are reduced by improving its efficiency while accounting for the fact that the remaining components are operating under real conditions:

$$\dot{E}_{D,k}^{AV,INT} = \dot{E}_{D,k} - \dot{E}_{D,k}^{MIN,k}. \qquad (3)$$

The avoidable exergy destruction within the k-th component, which is caused by the avoidable irreversibilities occurring within the r-th component (i.e., externally caused) ($\dot{E}_{D,k}^{AV,EXT,r}$), can be computed by subtracting the exergy destruction rate ($\dot{E}_{D,k}^{MIN,r}$) within the k-th component under the conditions at which the r-th component operates with reduced irreversibilities and the remaining components are operated under their real conditions from the exergy destruction rate ($\dot{E}_{D,k}$) occurring within the k-th component under its real operation conditions:

$$\dot{E}_{D,k}^{AV,EXT,r} = \dot{E}_{D,k} - \dot{E}_{D,k}^{MIN,r}. \qquad (4)$$

The importance of the components from the thermodynamic viewpoint and priorities for improving the k-th components were identified on the basis of the sum of the internally caused avoidable exergy destruction ($\dot{E}_{D,k}^{AV,INT}$) and the externally caused avoidable exergy destruction within the remaining components ($\dot{E}_{D,r}^{AV,EXT,k}$)

$$\dot{E}_{D,k}^{AV,\Sigma,INT,EXT} = \dot{E}_{D,k}^{AV,INT} + \sum_{\substack{r=1 \\ r\neq k}}^{n-1} \dot{E}_{D,r}^{AV,EXT,k} . \qquad (5)$$

2.2. Case Study

The investigated heat pump system was considered to be able to be reversed by means of a refrigerant change-over, which reverses the flow passage into the two exchangers (Figure 1). In cooling mode, the air-based heat exchanger (outside heat exchanger) worked as condenser, rejecting heat into the outdoor air, while the water-based heat exchanger (inside heat exchanger) worked as an evaporator, absorbing heat from the two-pipe water distribution system. In heating mode, the air exchanger worked as an evaporator, absorbing heat from outdoor air, while the water exchanger worked as a condenser, transferring heat into the same distribution system. It was assumed that the cold-emission terminal units were adapted for hot emission at low temperatures.

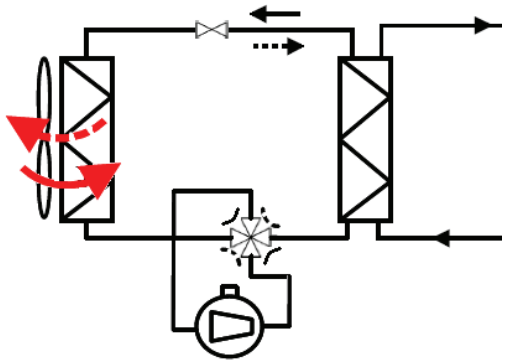

Figure. 1. Investigated reversible air-to-water unit connected to a two-pipe distribution system.

In heating mode the outside air was assumed to be cooled in the air-based heat exchanger from −7 °C down to −12 °C and the water was assumed to be heated in the condenser (water-based heat exchanger) from 40 °C up to 45 °C. In cooling mode the outside air was assumed to be heated in the outside heat exchanger (condenser) from 30 °C up to 35 °C and the chilled water was assumed to be cooled in the inside heat exchanger (evaporator) from 12 °C down to 7 °C. The pinch-point temperature in the outside and inside heat exchangers were taken as 12 K and 5 K, respectively. The pressure drop of the working fluids in the pipes and components was neglected.

In the design mode, which was used for sizing system, the following assumption were made:

- the evaporation temperature of R290 was calculated as the difference between the temperature of the secondary working fluid (air for heating mode and chilled water for cooling mode, respectively) at the evaporator outlet and the pinch point temperature difference in the evaporator (12 K or 5 K, respectively);
- the temperature of R290 at the compressor inlet was increased by 5 K due to superheating within the evaporator;
- the condensation temperature of R290 was calculated by adding the value of the pinch point temperature of the condenser (5 K or 12 K, respectively) to the temperature of the secondary working fluid (heated water or outside air, respectively) at the condenser outlet.

The specific power required by compressor was estimated from the following equation [3], [9]

$$l_{CM} = \frac{\left(h_{CM,in} - h_{CM,out}\right)}{\eta_{is}}, \qquad (6)$$

where η_{is} is the compressor's isentropic efficiency, and $h_{CM,in}$ and $h_{CM,out}$ are the specific enthalpies at the inlet and outlet of the compressor, respectively.

Specific enthalpy at the compressor outlet after real compression was calculated as

https://doi.org/10.52202/069564-0077

$$h_{CM,out} = h_{CM,in} + \frac{h_{CM,out,is} - h_{CM,in}}{\eta_{is}}, \qquad (7)$$

where $h_{CM,out,is}$ is the specific enthalpy at the compressor outlet after isentropic compression.

The volumetric (η_{vol}) and isentropic (η_{is}) efficiencies of the compressor were calculated using Pierre's correlations for "good" reciprocating compressors [10] following the methodology used in [11], [12]:

$$\eta_{vol} = k_1 \cdot \left(1 + k_s \cdot \frac{t_{CM,in} - 18}{100}\right) \cdot exp\left(k_2 \cdot \frac{p_{CM,in}}{p_{CM,out}}\right); \qquad (8)$$

$$\frac{\eta_{vol}}{\eta_{is}} = \left(1 + k_e \cdot \frac{t_{CM,in} - 18}{100}\right) \cdot exp\left(a \cdot \frac{T_1}{T_2} + b\right), \qquad (9)$$

where $t_{CM,in}$ is the refrigerant temperature at the compressor inlet, $p_{CM,in}/p_{CM,out}$ is the pressure ratio, T_1/T_2 is the ratio of the condensation and evaporation absolute temperatures (in Kelvin) corresponding to the discharge and the suction compressor pressures. The remaining symbols - k_1, k_s, k_2, k_e, a and b - are constants equal to 1.04, 0.15, −0.07, −0.1, −2.40, and 2.88, respectively.

The expansion valve was modelled as an isenthalpic component

$$h_{EXV,in} = h_{EXV,out}, \qquad (10)$$

where $h_{EXV,in}$, $h_{EXV,out}$ are the specific enthalpies at the inlet and outlet of the expansion valve, respectively.

Mass flow rate of R290 under design conditions in heating mode was calculated as

$$\dot{m}_{wf} = \frac{\dot{Q}_{Heat}^{Design}}{h_{CD,in} - h_{CD,out}}, \qquad (11)$$

where $\dot{Q}_{Heat}^{Design}$ is the heating load of the system at the design conditions, $h_{CD,in}$ is the specific enthalpy of the refrigerant at the condenser inlet (i.e. at the compressor outlet) and $h_{CD,out}$ is the specific enthalpy of the refrigerant at the condenser outlet.

And consequently, the heat transfer rate in the evaporator was calculated as

$$\dot{Q}_{EV} = \dot{m}_{wf}\left(h_{EV,out} - h_{EV,in}\right), \qquad (12)$$

where $h_{EV,out}$ and $h_{EV,in}$ are the specific enthalpies of R290 at the evaporator's outlet and inlet, respectively.

In cooling mode the mass flow rate of R290 was calculated by the following equation

$$\dot{m}_{wf} = \frac{\dot{Q}_{Cool}^{Design}}{h_{EV,out} - h_{EV,in}}, \qquad (13)$$

where $\dot{Q}_{Cool}^{Design}$ is the cooling load of the system at the design conditions, $h_{EV,out}$ is the specific enthalpy of the refrigerant at the evaporator outlet (at the compressor inlet) and $h_{EV,in}$ is the specific enthalpy of the refrigerant at the evaporator inlet (at the expansion valve outlet).

Hence, the heat transfer rate of the condenser was found as

$$\dot{Q}_{CD} = \dot{m}_{wf}\left(h_{CD,in} - h_{CD,out}\right). \qquad (14)$$

The power required by compressor was evaluated as

$$\dot{W}_{CM} = \dot{m}_{wf}\left(h_{CM,out} - h_{CM,in}\right). \qquad (15)$$

The compressor swept volume ($\dot{V}_s$) was estimated using the following equation

$$\dot{V}_s = \frac{\dot{m}_{wf} \upsilon_{CM,in}}{N \eta_{vol}}. \qquad (16)$$

where N is the compressor rotational speed, η_{vol} is the compressor's volumetric efficiency and $\upsilon_{CM,in}$ is the specific volume of R290 at the suction line of the compressor.

Mass flow rates of the secondary fluids through the heat exchangers were governed by the energy rate balance equations

$$\dot{m}_{air(water)} = \frac{\dot{Q}_{EV}}{\left(h_{air(water),in} - h_{air(water),out}\right)}; \qquad (17)$$

$$\dot{m}_{water(air)} = \frac{\dot{Q}_{CD}}{\left(h_{water(air),out} - h_{water(air),in}\right)}; \qquad (18)$$

where h_{air} and h_{water} are the specific enthalpies of the air and water at inlet (in) and outlet (out), respectively.

The condenser was divided into two main sections: the de-superheating region and the phase change region. The subcooled zone was neglected. The evaporator consisted of an evaporation region and a superheating one. The heat transfer rate within these sections was evaluated using the logarithmic mean temperature difference approach [3], [9]

$$\dot{Q} = U \cdot A \cdot LMTD, \qquad (19)$$

where $\dot{Q}$ is the heat transfer rate, U is the overall heat transfer coefficient, A is the heat transfer area of the considered section and $LMTD$ is the logarithmic mean temperature difference defined by the following equation

$$LMTD = \frac{\Delta T_2 - \Delta T_1}{ln\left(\frac{\Delta T_2}{\Delta T_1}\right)}, \qquad (20)$$

where ΔT_1 and ΔT_2 are temperature differences between the working fluids on the hot and cold sides at each end of the considered section.

For the air-based heat exchanger (finned-tube heat exchanger), the following expression for the overall heat transfer coefficient referring to secondary fluid heat transfer surface was applied

$$U = \left(\frac{1}{\alpha_{air}} + \frac{1}{\alpha_{wf}} \cdot \frac{A_{air}}{A_{wf}}\right)^{-1}, \qquad (21)$$

where A_{air} and A_{wf} are the heat transfer areas on the air and the refrigerant side, respectively, and α_{air} and α_{wf} are the corresponding heat transfer coefficients, respectively.

The plate heat exchanger was designed as the inside unit.

The data presented in [13], [14], [15] were generalized and used for calculation of the overall heat transfer coefficients within the specified condenser and evaporator regions.

The temperature and absolute pressure of the outside air were used to ascertain the thermodynamic properties at the evaporator inlet for heating mode and at the condenser inlet for cooling mode, respectively.

The thermo-physical properties of all the working fluids were evaluated via CoolProp [16]. The simulations were performed through MATLAB software package.

The same procedure was applied for the design of the system and estimation of internally and externally caused exergy destruction with pinch point temperatures in the air-based heat exchanger and the water-based heat exchanger equal to 6 K and 2 K, respectively and increased efficiency of the compressor by 10 % compared to real designed conditions.

After finding geometric parameters of the system, the operating characteristics were calculated for off-design conditions. During the off-design operations in heating mode, the water temperatures at the inlet and outlet of the water-based heat exchanger were equal to 40 °C and 45 °C, respectively. During cooling mode at the off-

https://doi.org/10.52202/069564-0077

design conditions, the water temperatures at the water-based heat exchanger's outlet and inlet were equal to 7 °C and 12 °C, respectively. Then, the mathematical approach suggested in [17] was adopted to assess the thermodynamic parameters of the investigated heat pumps under off-design conditions in both cooling and heating modes. During these calculations the mass flow rate of the working fluid was governed by the Eq. (16). Eq. (19) was used for the evaluation of either the heat transfer rates or the temperatures within considered heat transfer section.

As the main focus of this work is on the implementation of an exergetic evaluation, the overall heat transfer coefficients were considered as constant under off-design modes and equal to the ones estimated for the design mode.

The off-designed modes were estimated under real operation conditions and under conditions conducive to the evaluation of the removable exergy destruction.

Exergetic analysis was performed based on the selection of the ambient (outdoor) air parameters as the reference ones [18].

3. Results and Discussion

Heat transfer areas of the air- and water-based heat exchangers, which were required for covering heating or cooling loads by the inside heat exchanger, are presented in Figure 1. It could be observed that in general for covering cooling loads the air-based heat exchanger was found to be larger and the water-based heat exchanger was found to be smaller compared to the required heat transfer areas for covering the same heating loads with the same pinch point temperature. Also, the value of oversizing or undersizing depended on the ratios between heating and cooling loads ($\dot{Q}_{Heat}/\dot{Q}_{Cool}$), which then was found to affect the irreversibilities within the components.

For example, if the system had been sized with the specified pinch point temperature within heat exchangers on the base of heating design loads equal to 12 kW the area of the outside heat exchanger should have been 7.7 m^2 and the area of the inside heat exchanger should have been 2.2 m^2. However, for providing the same cooling load with the same pinch point temperature the heat transfer area of the outside and inside heat exchangers should have been 18.4 m^2 and 1.3 m^2, respectively. Thus, the system designed in this way would have had undersized area of the air-based heat exchanger for operation with 12 kW cooling load, which should have been compensated with larger temperature difference, leading to increased irreversibilities within the outside heat exchanger, expansion valve and compressor. On the other hand, the water-based heat exchanger of the system would have had oversized area for covering 12 kW cooling demand, which would have provided lower temperature difference within the heat exchanger and thus decreased irreversibilities within this component, expansion valve and compressor. The higher the ratios of heating demand to cooling one ($\dot{Q}_{Heat}/\dot{Q}_{Cool}$) for the system designed on the base of heating loads, the better agreement between the designed and required areas of the air-based heat exchanger and larger oversizing of the designed areas of water-based heat exchanger for covering cooling loads.

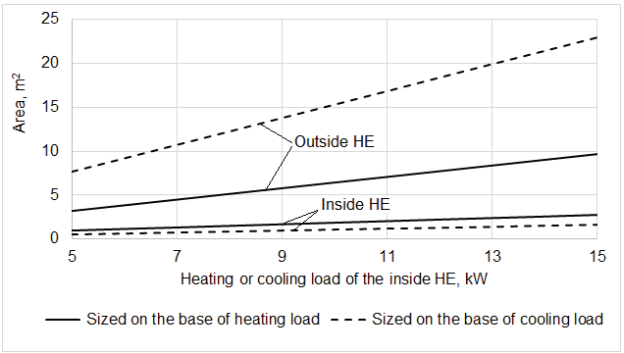

Figure. 2. Needed heat transfer areas for the air- and water-based heat exchangers required for covering the heating or cooling loads of the water-based heat exchanger.

If the system had been sized using a cooling design load of 10 kW, the areas of the outside and inside heat exchangers would have been equal to 15.3 m^2 and 1.1 m^2, respectively, and appropriate exergy destruction would have been obtained. In case of providing 10kW of heating load, due to oversized area of the air-based heat exchanger and undersized area of the water-based heat exchanger, this system would demonstrate other values of exergy destruction. For higher ratios $\dot{Q}_{Heat}/\dot{Q}_{Cool}$ of the system designed on the base of the cooling loads the degree of difference between the designed areas of the air-based heat exchanger and the needed

ones for covering heating loads would have been smaller. However, undersizing the water-based heat exchanger for covering heating loads would have been bigger.

The distribution of the exergy destruction rates in the components of the investigated system sized on the base of the heating design load with different ratios between heating and cooling loads ($\dot{Q}_{Heat}/\dot{Q}_{Cool}$) is shown in Figure 3. It could be seen that when the designed system was operated for covering cooling loads (empty circles in Figure 3a) at the ratios of heating loads to cooling ones ranging from 0.65 to 1.4 the air-based heat exchanger had much larger exergy destruction rates compared to the mode operated for covering heating loads (filled circles in Figure 3,a). This could be obtained due to undersized area of the outside heat exchanger, which was explained with the above suggestions (see Figure 2).

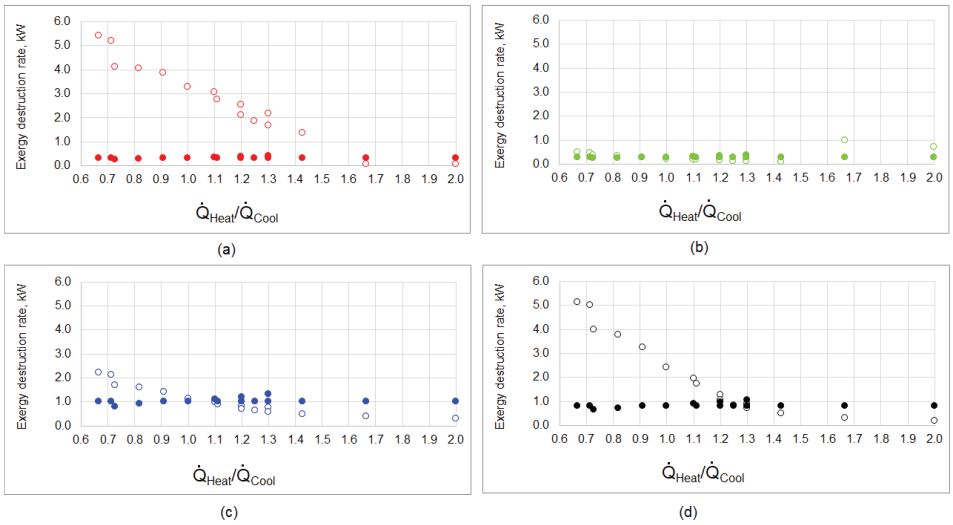

Figure. 3. Exergy destruction rates in the components of the system sized on the base of heating design loads with different ratios to heating loads and cooling ones: a) outside heat exchanger, b) inside heat exchanger, c) compressor, d) expansion valve, filled circles – operated for covering heating load, empty circles - operated for covering cooling load.

Oversized areas of the water-based heat exchanger did not change substantially exergy destruction rates within the inside heat exchanger operated for covering cooling loads (see Figure 3b).

At the ratios of heating loads and cooling ones ranging from 0.65 to 1.4 temperature differences in the air-based heat exchanger was increased. As a result, it provided higher pressure ratios in the compressor and the expansion valve. The exergy destruction within these components was incresed (empty circles in Figure 3c and Figure 3d) in comparison to heating modes (filled circles in Figure 3c and Figure 3d).

If the system had been sized on the base of the cooling design loads (Figure 4) it could not have been operated for the values of $\dot{Q}_{Heat}/\dot{Q}_{Cool}$ higher than 1.3 due to technological limitations. Similarly to the previous scenario, in case of sizing system based on cooling design loads the outside heat exchanger would have been oversized for covering heating loads, resulting in decreased exergy destruction rates (filled circles in Figure 4a) within this component compared to the cooling modes (empty circles in Figure 4a). For $\dot{Q}_{Heat}/\dot{Q}_{Cool}$ values higher than 0.8, in case of the use of an undersized water-based heat exchanger during heating modes, the exergy destruction rates would have been higher (filled circles in Figure 4b) than during cooling modes (empty circles in Figure 4b). As it was said above, oversized and undersized areas led to a decrease and an increase of temperature driving force for heat transfer (temperature differences) and pressure ratios, respectively. As a result, exergy destruction rates within compressor and expansion valve in heating mode (filled circles in Figure 4c and Figure 4d) were found to be larger than during cooling modes (empty circles in Figure 4c and Figure 4d).

https://doi.org/10.52202/069564-0077

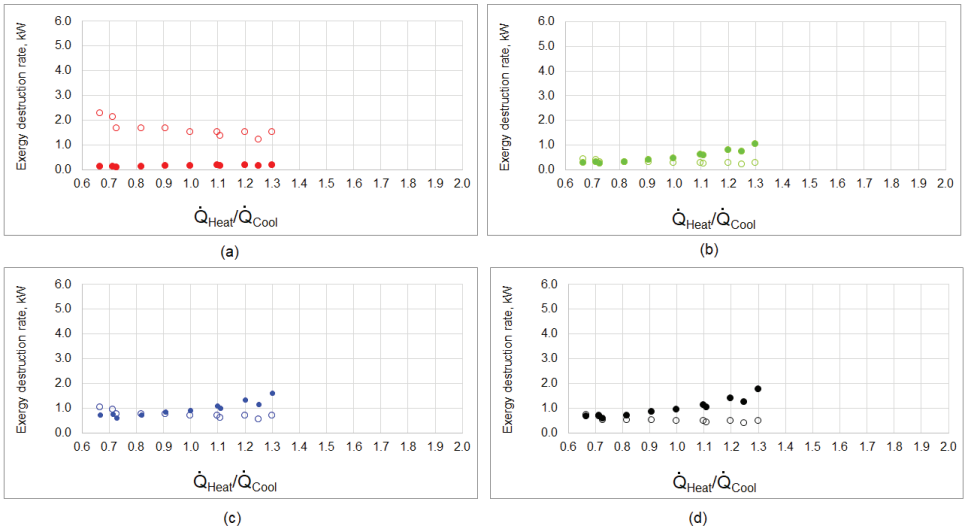

Figure. 4. Exergy destruction rates in the components of the system sized on the base of cooling design loads with different ratios of heating loads and cooling ones: a) outside heat exchanger, b) inside heat exchanger, c) compressor, d) expansion valve, filled circles – operated for covering heating load, empty circles - operated for covering cooling load.

The values of the total exergy destruction rates in the system with different ratios of heating loads and cooling ones are shown in Figure 5.

It was found that for the ratios of heating loads and cooling ones within the range 0.65 to 1.2 the system should have been sized based on the cooling loads. For such design lower total exergy destruction within the system could have been obtained (from 4.5 kW to 6.5 kW) compared to the system sized on the base of heating loads, which demonstrated higher total exergy destruction (from 12.0 kW to 6.5 kW).

As the ratios of heating design loads and cooling ones were higher than 1.2, the heating design load should have been used for sizing the system components. Under such design conditions thermodynamic efficiency of the system was substantially decreased.

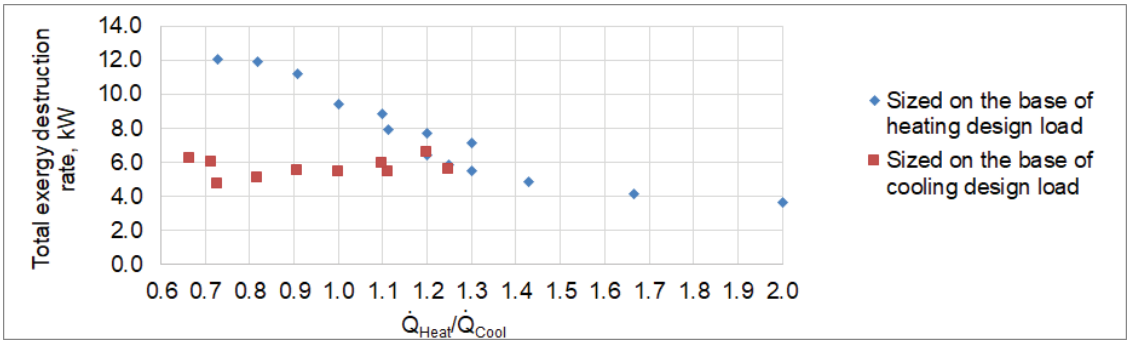

Figure. 5. Total exergy destruction rates in the system with different ratios between heating and cooling loads.

The values of the removable and internally caused exergy destruction rate within the k-th component ($\dot{E}_{D,k}^{AV,INT}$) and that of the removable and externally caused exergy destruction rate within the remaining components caused by the k-th component ($\dot{E}_{D,r}^{AV,EXT,k}$) for the system designed on the base of heating load are presented in Figure 6. The system was operated for covering 10 kW and 7 kW of heating and cooling loads, respectively.

It was observed from Figure 7 that 0.44 kW of removable exergy destruction rate in the compressor could be reduced by improving this component. Another smaller part of removable exergy destruction rate in the compressor was caused by the irreversibilities that occurred in the remaining components: inside heat exchanger (i.e. 0.07 kW) and outside heat exchanger (0.29 kW). Also, 0.11 kW of removable exergy destruction rate within the inside heat exchanger could be reduced by decreasing the irreversibilities within this component. Another part of removable exergy destruction rate within the water-based heat exchanger

(0.06 kW) could be eliminated by improving the remaining components (i.e. compressor and air-based heat exchanger). The results obtained from the proposed methodology indicated that the internally caused and removable exergy destruction rate in the expansion valve was zero. This means that the exergy destruction rate within this component could be reduced through the enhancement in the remaining components. The inside heat exchanger was found to be responsible for 0.12 kW of exergy destruction rate, which could be removed within the expansion valve. In addition, 0.38 kW of removable exergy destruction rate within the expansion valve were caused by irreversibilities within outside heat exchanger. Furthermore, 0.04 kW of removable exergy destruction rate within the expansion valve depended on irreversibilities taking place in the compressor. According to the results presented in Figure 6 the largest value of exergy destruction rate, which could be removed in the air-based heat exchanger, was internally caused (0.62 kW). Furthermore, 0.12 kW and 0.05 kW of avoidable exergy destruction within the outside heat exchanger depended on irreversibilities taking place in the compressor and the inside unit, respectively.

Therefore, according to the results obtained the highest priority for improvement of the considered system had to be given to the air-based heat exchanger. This was due to the fact that the sum of the internally caused and the externally caused exergy destruction rates, which could be avoided within the investigated heat pump with the help of improving this component, was the highest one and equal to 1.32 kW (i.e. 58 %) (Figure 6). Secondly, the investigator needed to focus on the compressor, being accountable for 0.63 kW (i.e. 27 %) of avoidable exergy destruction within the evaluated system. Thirdly, the water-based heat exchanger enhancement was found to lead to a potential decrease of 0.35 kW (i.e. 15 %) of exergy destruction.

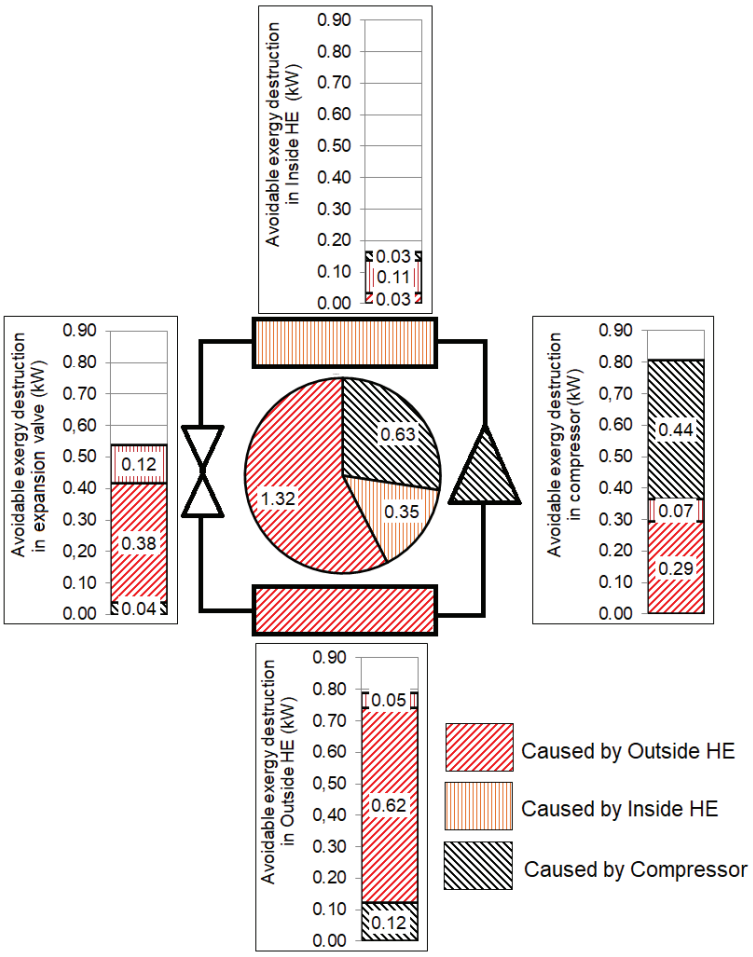

Figure. 6. Values of the internally caused and externally caused avoidable exergy destruction rates (kW) in the components of the R290 air-to-water reversible heat pump designed on the base of heating load and operated for covering 10kW and 7kW of heating and cooling loads, respectively.

Compared to the results obtained from the previous case, slightly different values of the avoidable exergy destruction were evaluated within the studied system designed on the base of cooling load (see Figure 7). The

https://doi.org/10.52202/069564-0077

system was operated for covering 8kW and 11kW of heating and cooling loads. The major differences were found to be associated with the avoidable parts of exergy destruction caused by the outside heat exchanger.

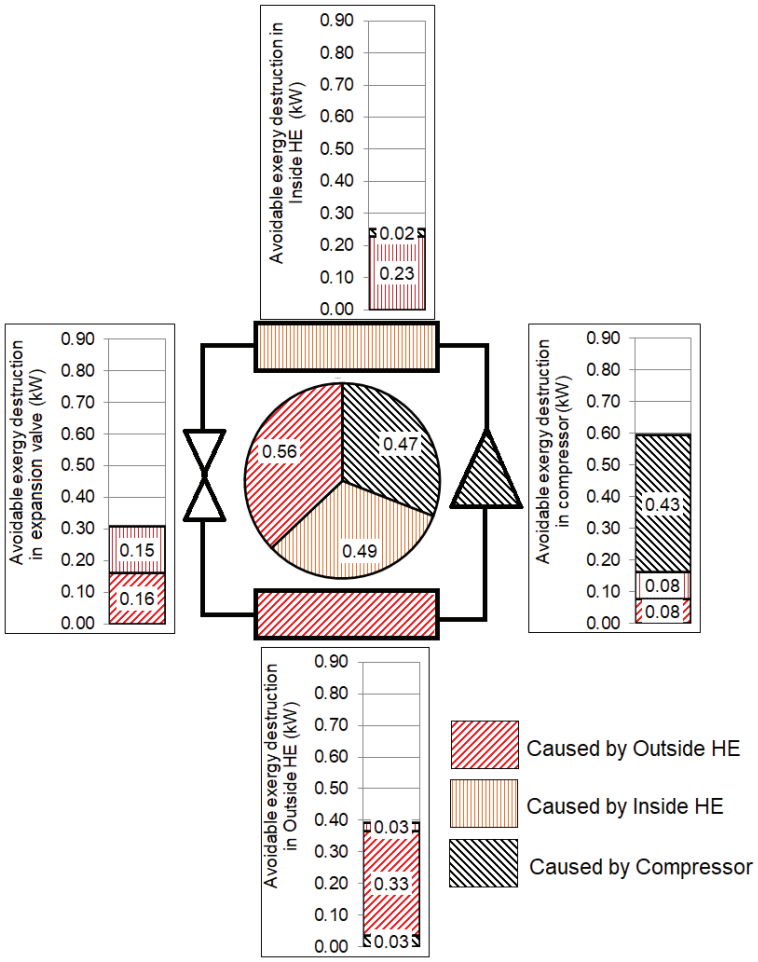

Figure. 7 Values of the internally caused and externally caused avoidable exergy destruction rates (kW) in the components of the R290 air-to-water reversible heat pump designed on the base of cooling load and operated for covering 8 kW and 11 kW of heating and cooling loads, respectively.

The impact of irreversibilities within the outside heat exchanger was decreased. As a result, the outcomes obtained showed that the outside, inside heat exchanger and the compressor had almost the same priority for improvement. The air-based heat exchanger revealed 0.56 kW avoidable exergy destruction within the system. Also, the water-based heat exchanger offered the potential to reduce 0.49 kW of exergy destruction rate. Also, the compressor enhancement was found to lead to a potential decrease of 0.47 kW of exergy destruction within the investigated system.

Conclusions

An exergy-based analysis has been carried out to evaluate the impact of different ratios between heating and cooling loads on the thermodynamic efficiency of a reversible air-to-water system with propane for providing heating and cooling needs. The following major findings have been found:

- For the system sized using heating design loads undersizing and oversizing areas of the air-based and water-based heat exchangers were obtained, respectively, for covering the same cooling loads with the same pinch-point temperature differences and vice versa;
- Such disagreement of designed and required heat transfer areas affect the distribution of irreversibilities within the components of the system significantly, mainly depending on the ratios between heating and cooling loads and the way of system design (based on heating or cooling load);
- It has been found that for the ratios of heating loads and cooling ones within the range from 0.65 to 1.2 the system should be sized based on the cooling loads. For such design approach lower total

exergy destruction within the system could be obtained compared to the system sized on the base of heating loads. As the ratios of heating loads and cooling ones are higher than 1.2, the heating design load should be used for sizing system components. This is because the system designed on the base of cooling load could not be operated for covering heating needs due to technological limitations.

- For the system sized on the base of heating loads removing the avoidable irreversibilities within the air-based heat exchanger offer the biggest decrease of the exergy destruction within the system;
- thermodynamic improvement of the air-based, water-based heat exchanger and the compressor have approximately the same potential for increasing efficiency of the system designed on the base of cooling loads.

Acknowledgments

This research was funded by Ministry of Education and Science of Ukraine, grant number 0122U001750.

Nomenclature

A heat transfer area (m^2)

$\dot{E}$ exergy rate (W)

$\dot{Q}$ heat transfer rate (W)

h specific enthalpy (J/kg)

k_1, k_s, k_2, k_e, a and b Pierre's correlations constants

$\dot{m}$ mass flow rate (kg s^{-1})

N rotational speed (s^{-1})

P absolute pressure (Pa)

s specific entropy (J/(kg·K))

T temperature (K)

U overall heat transfer coefficient (W m^{-2} K^{-1})

V volume (m^3)

υ specific volume (m^3/kg)

$\dot{W}$ shaft power required by compressor (W)

GWP global warming potential

HFC hydrofluorocarbon

HFO hydrofluoroolefin

HVAC heating, ventilation, and air-conditioning

$LMTD$ logarithmic mean temperature difference (K)

Subscripts and superscripts

air air

CD condenser

CM compressor

D destruction

EXT external

EXV expansion valve

EV evaporator

F fuel

gen generation

INT, int internal

is isentropic

in inlet

k k-th component

MIN minimum

out outlet

P product

r r-th component

https://doi.org/10.52202/069564-0077

ref refrigerant

s swept

vol volumetric

water water

wf working fluid

$_0$ reference state

Greek symbols

α convection heat transfer coefficient (W m^{-2} K^{-1})

η efficiency (-)

References

1. Stabat, P.; Marchio, D. Opportunities for Reversible Chillers in Office Buildings in Europe. *Build. Simul.* **2009**, *2*, 95–108, doi:10.1007/S12273-009-9207-z.
2. Dongellini, M.; Naldi, C.; Morini, G.L. Sizing Effects on the Energy Performance of Reversible Air-Source Heat Pumps for Office Buildings. *Applied Thermal Engineering* **2017**, *114*, 1073–1081, doi:10.1016/j.applthermaleng.2016.12.010.
3. Kinab, E.; Marchio, D.; Rivière, P.; Zoughaib, A. Reversible Heat Pump Model for Seasonal Performance Optimization. *Energy and Buildings* **2010**, *42*, 2269–2280, doi:10.1016/j.enbuild.2010.07.007.
4. Madonna, F.; Bazzocchi, F. Annual Performances of Reversible Air-to-Water Heat Pumps in Small Residential Buildings. *Energy and Buildings* **2013**, *65*, 299–309, doi:10.1016/j.enbuild.2013.06.016.
5. Nawaz, K.; Shen, B.; Elatar, A.; Baxter, V.; Abdelaziz, O. R1234yf and R1234ze(E) as Low-GWP Refrigerants for Residential Heat Pump Water Heaters. *International Journal of Refrigeration* **2017**, *82*, 348–365, doi:10.1016/j.ijrefrig.2017.06.031.
6. Nawaz, K.; Shen, B.; Elatar, A.; Baxter, V.; Abdelaziz, O. R290 (Propane) and R600a (Isobutane) as Natural Refrigerants for Residential Heat Pump Water Heaters. *Applied Thermal Engineering* **2017**, *127*, 870–883, doi:10.1016/j.applthermaleng.2017.08.080.
7. Bejan, A.; Tsatsaronis, G.; Moran, M.J. *Thermal Design and Optimization*; Wiley: New York, 1996; ISBN 978-0-471-58467-4.
8. Voloshchuk, V.; Gullo, P.; Nikiforovich, E. A New Approach for Estimation of Avoidable Exergy Destruction: A Case Study of a Heat Pump Unit. *In Proceedings of the 34th International Conference on Efficency, Cost, Optimization, Simulation and Envi-ronmental Impact of Energy Systems (ECOS'21),* **2021**, 1369–1377.
9. Sanaye, S.; Chahartaghi, M.; Asgari, H. Dynamic Modeling of Gas Engine Driven Heat Pump System in Cooling Mode. *Energy* **2013**, *55*, 195–208, doi:10.1016/j.energy.2013.03.074.
10. Granryd E.; Ekroth I.; Lundqvist P.; Melinder A.; Palm B.; Rohlin P. *Refrigeration Engineering*; K. Tek. Högskolan, 1999;
11. Mateu-Royo, C.; Sawalha, S.; Mota-Babiloni, A.; Navarro-Esbrí, J. High Temperature Heat Pump Integration into District Heating Network. *Energy Conversion and Management* **2020**, *210*, 112719, doi:10.1016/j.enconman.2020.112719.
12. Mateu-Royo, C.; Navarro-Esbrí, J.; Mota-Babiloni, A.; Amat-Albuixech, M.; Molés, F. Thermodynamic Analysis of Low GWP Alternatives to HFC-245fa in High-Temperature Heat Pumps: HCFO-1224yd(Z), HCFO-1233zd(E) and HFO-1336mzz(Z). *Applied Thermal Engineering* **2019**, *152*, 762–777, doi:10.1016/j.applthermaleng.2019.02.047.
13. Botticella, F.; Viscito, L. Seasonal Performance Analysis of a Residential Heat Pump Using Different Fluids with Low Environmental Impact. *Energy Procedia* **2015**, *82*, 878–885, doi:10.1016/j.egypro.2015.11.832.
14. Longo, G.A. Heat Transfer and Pressure Drop during Hydrocarbon Refrigerant Condensation inside a Brazed Plate Heat Exchanger. *International Journal of Refrigeration* **2010**, *33*, 944–953, doi:10.1016/j.ijrefrig.2010.02.007.
15. Amalfi, R.L.; Vakili-Farahani, F.; Thome, J.R. Flow Boiling and Frictional Pressure Gradients in Plate Heat Exchangers. Part 1: Review and Experimental Database. *International Journal of Refrigeration* **2016**, *61*, 166–184, doi:10.1016/j.ijrefrig.2015.07.010.
16. Bell, I.H.; Wronski, J.; Quoilin, S.; Lemort, V. Pure and Pseudo-Pure Fluid Thermophysical Property Evaluation and the Open-Source Thermophysical Property Library CoolProp. *Ind. Eng. Chem. Res.* **2014**, *53*, 2498–2508, doi:10.1021/ie4033999.
17. Herbas, T.B.; Berlinck, E.C.; Uriu, C.A.T.; Marques, R.P.; Parise, J.A.R. Steady-State Simulation of Vapour-Compression Heat Pumps. *Int. J. Energy Res.* **1993**, *17*, 801–816, doi:10.1002/er.4440170903.
18. *Exergy Assessment Guidebook for the Built Environment: ECBCS Annex 49 - Low Exergy Systems for High-Performance Buildings and Communities*; Torío, H., Fraunhofer-Institut für Bauphysik, Eds.; Fraunhofer Verlag: Stuttgart, 2011; ISBN 978-3-8396-0239-3.